The 33rd Annual Conference of the IEEE Industrial Electronics Society (IECON)
Nov. 5-8, 2007, Taipei, Taiwan

DSP-Based Auto-Tuning Design of Permanent Magnet Synchronous Motor Drives

Ming-Shyan Wang, Tzu-Chang Shau, and Chia-Ming Chang
Department of Electrical Engineering, Southern Taiwan University of Technology
E-mail: mswang@mail.stut.edu.tw

Abstract- **The paper proposes an auto-tuning algorithm for a DSP-based permanent magnet synchronous motor (PMSM) drive. In order to be compatible with the conventional drives, the proportional-plus-integral (PI) speed control with gains individually designed by Bode diagram and an extension of the frequency-zone method to decouple the tuning gains in a multi-loop control system is studied. The auto-tuning scheme includes two steps, an adaptive load observer to estimate the load inertia and adaptive two-degree-of-freedom PI tuning. Finally, the experimental results of estimating some known inertia loads and square wave speed responses have verified the effectiveness of the proposed auto-tuning algorithm.**

I. INTRODUCTION

Nowadays the brushless servomotors play a fundamental role in manufacturing automation, such as robotics, hybrid vehicles, electric scooters, elevators, and fitness machines, etc. They can be constructed with either sinusoidal or trapezoidal back electromotive force (EMF) waveforms. The former machine is called permanent magnet synchronous motor (PMSM) and widely recognized to be preferable for high-performance servo applications on speed and position control systems [1]. A high-performance PMSM drive generally requires estimation of moment of inertia of the whole system including the motor and the load because variation of load inertia will degrade drive's performance. As a result, there exists a growing demand to automatically tune or self-tune the gain parameters according to varying operating conditions, especially on inertia and load torque varying overtime.

There were many papers on the estimation of system inertia for auto-tuning of speed-controlled motor drives. The auto-tuning methodology may be cataloged into two kinds, model-free method and model-based analytic method [2]. These reports based on model analytic method include approaches of gain and phase margins [3], adaptive control [4], observer-based control [5-6], and their combinations. The expert system and fuzzy control [7-10] have been built to perform gain tuning according to step-based or cycle-based information for a model-free strategy. Based on the advanced control theory, the servo system can have a desired time and/or frequency characteristics at the sacrifice of often becoming a high-order servo system such that it cannot sometimes be realized because of a smaller sampling time, a finite digital word length and a quantization error [11]. In addition, robust velocity-tracking for a mechanical system characterized by variable load torque and inertia, simplicity, and low cost are the main control objects of a speed loop according to industrial requirements [12]. However, proportional-integral-derivative (PID) controller not only has gained its popularity due to its meaningful physical interpretation but also is extensively used in practical applications [13-14]. As a result, in order to be conventionally compatible with the drives, the PID control is considered in the paper.

In the paper, a digital signal processor (DSP)-based PMSM drive is designed and implemented. An extension of the frequency zone-based method [15] is used to decouple the multiple tuning gains in a multi-loop control system for PMSM drives so that the gains may be adjusted individually. Then, by gradient approach, the auto-tuning design based on adaptive load observer and gain tuning is proposed. The paper is divided into four branches with further discussion as follows: Section 1, the introduction; section 2, PMSM drive and auto-tuning design; section 3, experimental results, and; section 4, conclusions.

II. DRIVE DESIGN AND AUTO-TUNING

Considering the Park and Clarke transformations, the dq-axis representation of a surface-mounted PMSM will be [1]

$$\begin{bmatrix} v_d \\ v_q \end{bmatrix} = \begin{bmatrix} R_s + pL_s & -\omega_{re}L_s \\ \omega_{re}L_s & R_s + pL_s \end{bmatrix} \begin{bmatrix} i_d \\ i_q \end{bmatrix} + \begin{bmatrix} 0 \\ e_q \end{bmatrix}, \qquad (1)$$

where R_s is the stator resistance, p represents the operator d/dt, L_s is the phase inductance, θ_{re} is electric angle between stator axis and rotor axis, $\omega_{re} = d\theta_{re}/dt$ is the electric speed, and $e_q = \omega_{re}\lambda_{af}$ is q-axis back EMF, where λ_{af} is the flux linkage due to the rotor magnet linking the stator.

Fig. 1 shows three relating current, speed, and position loops in a servo drive system. The detailed block diagram of current control is disclosed in Fig. 2. The space vector pulse-width modulation (SVPWM) is employed to supply different phase volts and operating frequencies to PMSM. Owing to the fast dynamics of current controller, a current source inverter can be

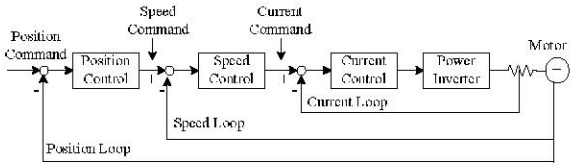

Fig. 1. Block diagram of a PMSM drive.

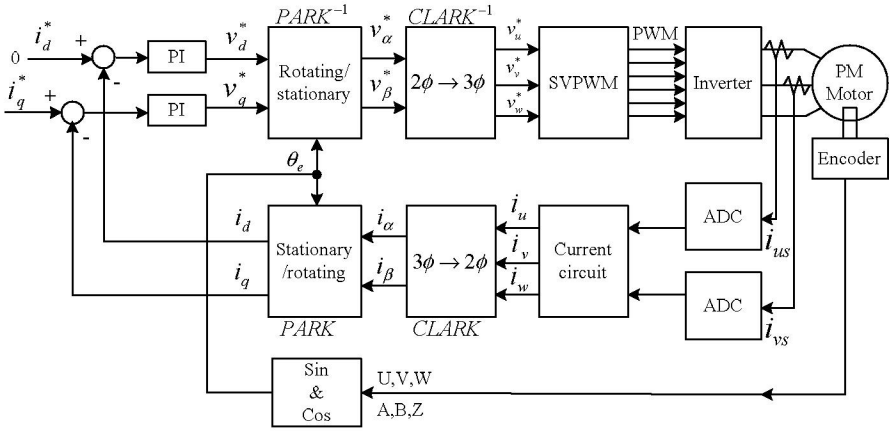

Fig. 2. Detailed block diagram of current control.

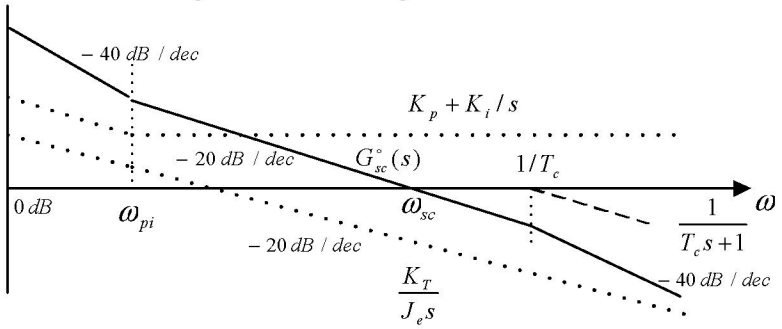

Fig. 4. Bode diagram of PI control.

assumed and the simple first-order model can be based on the speed controller design [12]. That is, after an inner loop is designed, it acts like a first-order low-pass filter within the outer loop. The inner loops operate in the next higher frequency zone to the outer loop. An extension of the frequency zone-based method will decouple the multiple tuning gains so that they may be adjusted individually [15]. Fig. 3 is the speed control block diagram where J_M, K_T, and $1/(1+T_c s)$ represent the motor inertia, torque constant, and the simplified model of current control loop, respectively.

The conventional PI control is applied to get zero steady-state error of speed,

$$G_s(s) = K_p + K_i/\mathrm{s} \ . \tag{2}$$

On the Bode plot of speed control loop shown in Fig. 4, the frequency range is divided into four zones by ω_{pi}, ω_{sc}, and $1/T_c$, where ω_{sc} is the designed gain-crossover frequency of the speed control loop and $\omega_{pi} = K_i / K_p$. If the ratios of

$$\omega_{sc} / \omega_{pi} = \alpha \ \text{ and } \ 1/(T_c \omega_{sc}) = \beta \tag{3}$$

are large enough, the magnitude of the open-loop transfer function in the medium frequency range around ω_{sc} may be approximated as

$$\left| G_{sc}^{\circ}(s) \right| = \left| G_s(s) \frac{1}{1+T_c s} \frac{K_T}{J_e s} \right| \approx \left| \frac{K_p K_T}{J_e s} \right| , \tag{4}$$

where J_e is the sum of J_M and reflected inertia from load. The gains will be functions of ω_{sc} and can be expressed by the following equations

$$K_p = J_e \omega_{sc} / K_T \ , \qquad K_i = J_e \omega_{sc}^2 / (\alpha K_T) \ . \tag{5}$$

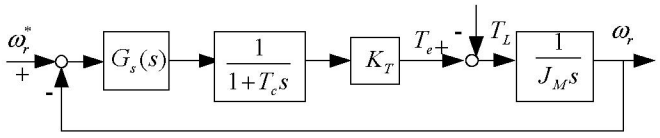

Fig. 3. Block diagram of speed control.

It is seen that, once ω_{sc} is chosen, K_p and K_i are adjusted according to the load.

The loads in industry applications are generally unknown or hard to be exactly found so that gains of K_p and K_i are tuned by senior engineers or auto-tuning function of drives. We will apply the adaptive law to estimate the load then tune the gains in term of a respective performance index, $E(k)$. By gradient method, make the back-difference of E with respect to a parameter vector $\mathbf{P} = [p_1 \ p_2 \ldots \ p_z]$ such that

$$p_i(t+1) = p_i(t) - \gamma_i \Delta E / \Delta p_i , \quad (i = 1, \ldots, z) , \tag{6}$$

where t, $\Delta E / \Delta p_i$, and γ_i $(0 < \gamma_i < 1)$ represent the number of learning, performance index variation with respect to parameter p_i, and learning rate, respectively. Based on the programming simplicity, the cost function E in auto-tuning process includes the percent of the maximum overshoot M_o and rise time t_r such that

$$E(k) = \zeta_{M_o} \cdot \left| M_{od} - M_o \right| + \zeta_{t_r} \cdot \left| t_{rd} - t_r \right| , \tag{7}$$

$$\begin{cases} \varsigma_{M_o} + \varsigma_{t_r} = 1 \\ 0 \le \varsigma_{M_o} \le 1 \\ 0 \le \varsigma_{t_r} \le 1 \end{cases},$$

$$\begin{aligned} K_p(k) &= K_p(k-1) - \mu_p E(k-1)/K_p(k-1) \\ K_i(k) &= K_i(k-1) - \mu_i E(k-1)/K_i(k-1) \end{aligned} \quad (8)$$

where ς_{M_o} and ς_{t_r} are the weighting factors, M_{od} and t_{rd} are the target values, and μ_p and μ_i are adjusting rates. However, the tuning trajectories shown in Fig. 5 have the constraints of

$$\begin{cases} K_p(\min) \le K_p \le K_p(\max) \\ K_i(\min) \le K_i \le K_i(\max) \end{cases} \quad (9)$$

such that the gains during tuning process must stabilize the controlled system. This is so-called two-degree-of-freedom (2DOF) PI tuning [13, 14, 16].

In addition, the load is another important parameter during auto-tuning process. Referring to Fig.6, the output of the adaptive observer is

$$\hat{\omega}_r = \int (\hat{K}_T i_q / \hat{J}_e) dt . \quad (10)$$

We define the performance index as the difference between observed speed and measured speed such that

$$\hat{J}_e(k) = \hat{J}_e(k-1) - \mu_J \Delta(\hat{\omega}_r - \omega_r)/\Delta\hat{J}_e . \quad (11)$$

However, the load estimation is not executed until the measured speed is less than a predefined speed, $\omega_{threshold}$, since q-axis current is very small during steady-state operation, shown in Fig. 7.

III. Experimental Results

A PMSM with parameters revealed in Table I coupled an incremental encoder with a resolution of 2000 pulse/revolution is employed in the experiment. The drive consists of a DSP TMS320F2407 and a control board that includes DC to DC converters, intelligent power module (IPM), current transducers, and protection circuit. MATLAB simulation verifies that α=5 and β=5 in (3) are appropriate values. For $J_L = 5.18 J_M$, speed sampling time $T_s = 200\mu s$ and $1/T_c = 4500\, rad/s$, Fig. 8 results the 3000 rpm step responses with rise times of 129, 59, and 39 ms for K_p=0.2 and $K_i = 36$ by (5) and torque limits of T_R, $2T_R$, and $3T_R$, respectively. Fig. 9 discloses the excellent linearity between the speed command within the rated-speed region (3000 rpm CW ~ 3000 rpm CCW) and the motor speed (upper) and the correspondence at low-speed region around zero speed (lower).

An adaptive observer shown in Fig. 6 based on a preset threshold motor speed is used to estimate eight load ratios J_L / J_M of 1, 5.18, 8.85, 13.05, 17.70, 28.30, 30.20, and 38.95.

TABLE I
PARAMETERS of PMSM 7CB30

Output power	300 W	Back EMF constant	54.9 V/Krpm
Torque	0.95 Nm	Inertia	0.224 Kgcm^2
Rated current	2.0 A	Stator resistance	2.79 Ω
Rated velocity	3000 RPM	Stator inductance	5.80 mH
Torque constant	0.524Nm/A		

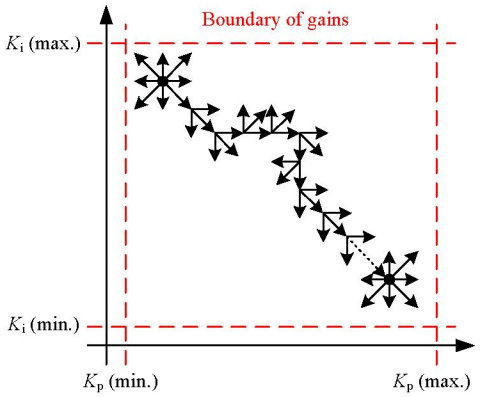

Fig. 5. 2DOF $K_p - K_i$ plane.

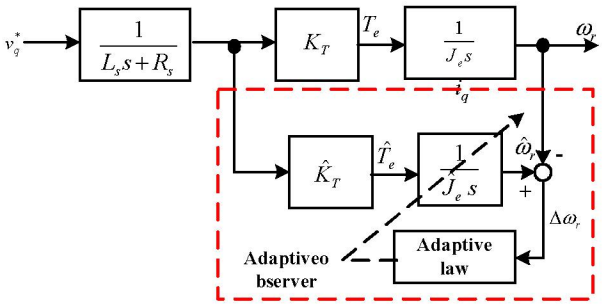

Fig. 6. Adaptive observer.

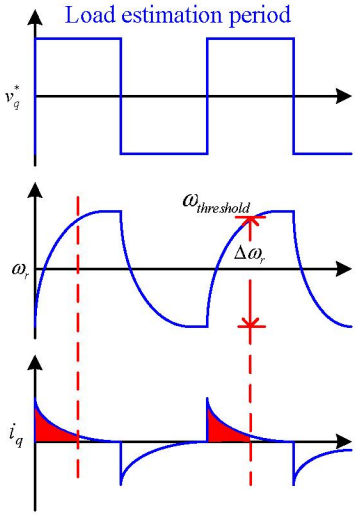

Fig. 7. Inertia estimation operation.

The observed load ratios shown in Fig. 10 are estimated under the conditions of three different thresholds, 100, 150, and 200 rpm, q-axis voltage of 45 V, and $\mu_J = 0.1$ in (11). It is satisfied for the estimated curves by comparing them with the actual curve. For $M_o = 10\%, t_r = 75ms$, $\varsigma_{M_o} = \varsigma_{t_r} = 0.5$, and $\mu_p = \mu_i$ =0.1, a square wave velocity command between 300 rpm to -300 rpm with a period of 4 seconds is considered for adaptive auto-tuning. Fig. 11 displays the responses for each ratio, in where the dash lines mean the transition from inertia estimation to auto-tuning control. These figures show good performance of transient and steady-state response. Fig.

12 depicts the speed responses tested by default gains then immediately tuned gains after load ratio estimation of 30.20 to compare the results. These results show the effectiveness of designed auto-tuning.

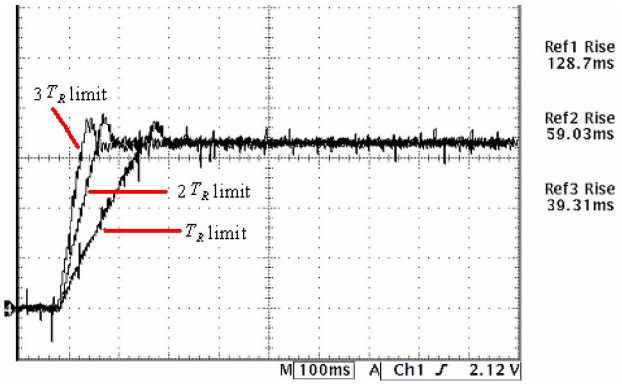

Fig. 8. Step responses of 3000 rpm with T_R, $2T_R$, and $3T_R$ limits.

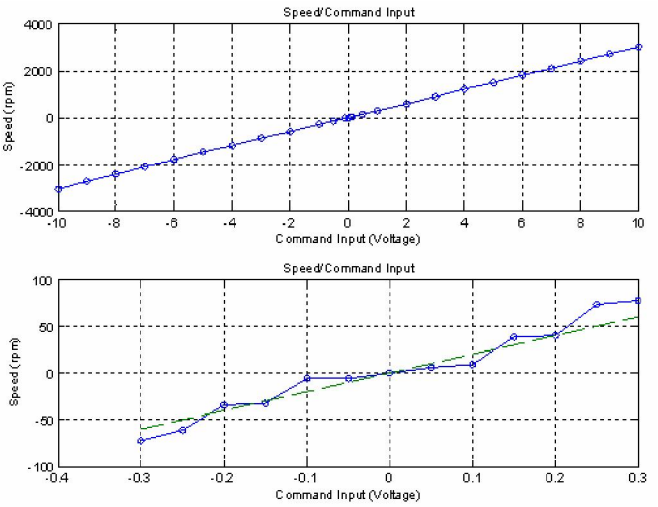

Fig. 9. Relation between speed input and command output.

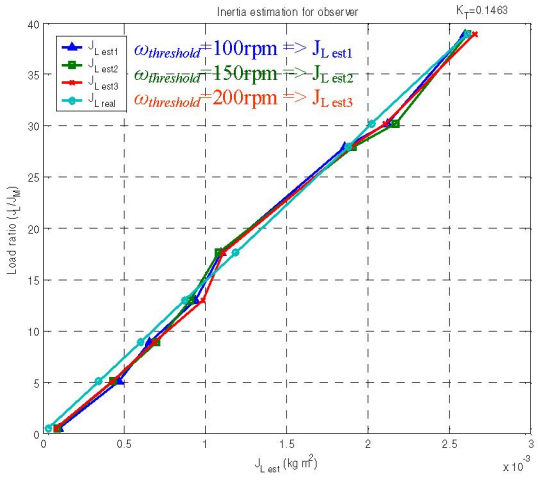

Fig. 10. Estimated load ratios.

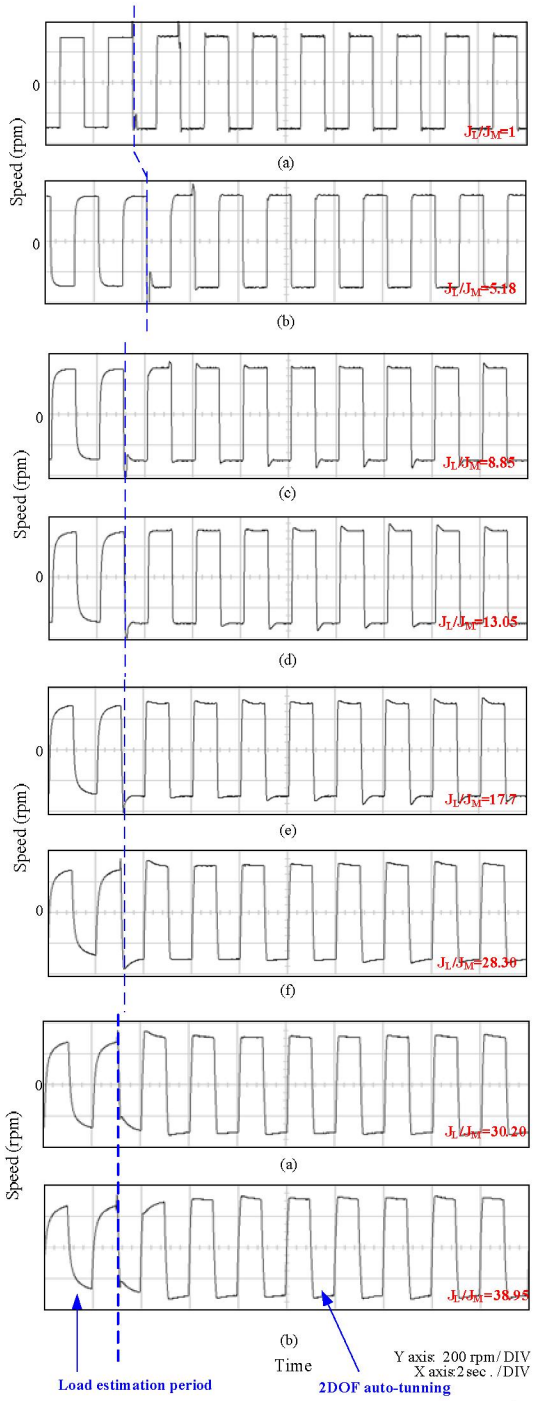

Fig. 11. Speed responses after load estimation, (a) $J_L/J_M = 1$, (b) $J_L/J_M = 5.18$, (c) $J_L/J_M = 8.85$, (d) $J_L/J_M = 13.05$, (e) $J_L/J_M = 17.7$, (f) $J_L/J_M = 28.30$, (g) $J_L/J_M = 30.20$, and (h) $J_L/J_M = 38.95$.

IV. CONCLUSIONS

The paper has developed an adaptive auto-tuning algorithm for a digital PMSM DSP-based drive. The PI speed control gains are individually given based on Bode diagram and an extension of the frequency-zone method that decouples the

tuning gains in a multi-loop control system. It has been shown that the drive has fast rise time for different torque limits. Known inertias have been first accurately estimated by a proposed adaptive load observer. Then, the PI gains have been adjusted by 2DOF adaptive auto-tuning algorithm. Finally, the experimental results have verified the effectiveness of the proposed auto-tuning algorithm.

ACKNOWLEDGMENT

The authors would like to express their appreciation to NSC for support under contact NSC 93-2622-E-218-018-CC3.

REFERENCES

[1] P. Pillay and R. Krishnan, "Application characteristics of permanent magnet synchronous and brushless DC motors for servo drives," *IEEE Trans. on Ind. Appl.* vol. 37, pp. 986-996, 1991.

[2] A. A. El-Samahy, M.A. El-Sharkawi, and S. M. Sharaf, "Adaptive multi-layer self-tuning high performance tracking control for DC brushless motor," *IEEE Trans. on Energy Convers.*, vol. 9, pp. 311-316, 1994.

[3] G.-S. Kim and M.-J. Youn, "Approximate gain-phase margin PI controller for direct drive PM synchronous motors," *Electronics Letters*, vol. 38, no. 23, pp. 1487– 1489, Nov. 2002.

[4] T. Higashiyama, M. Mine, H. Ohmori, A. Sano, H. Nishida, and Y. Todaka, "Auto-tuning of motor drive system by simple adaptive control approach," *Proceedings of the 2000 IEEE International Conference on Control Applications*, pp. 868-873, 25-27 Sept. 2000.

[5] S.-M. Yang and Y.-J. Deng, "Observer-based inertial identification for auto-tuning servo motor drives," *Fourtieth IAS Annual Meeting of Industry Applications Conference,* Vol. 2, pp. 968-972, 2-6 Oct. 2005.

[6] S. Kobayashi, I. Awaya, H. Kuromaru, and K. Oshitani, "Dynamic model based auto-tuning digital servo driver," *IEEE Trans. on Industrial Electronics*, vol. 42, no. 5, pp. 462–466, Oct. 1995.

[7] C. H. Tsai, C. H. Wang, and W. S. Lin, "Robust fuzzy model-following control of robot manipulators," *IEEE Trans. on Fuzzy Systems*, vol. 8, pp. 462-469, 2000.

[8] S. L. Ho, M. R. Fei, K. W. E. Cheng, and H.C. Wong, "An auto-tuning algorithm for the IRBF network of brushless DC motor," *IEEE Trans. on Magnetics,* vol. 40, no. 2, Part 2, pp. 1168–1171, Mar. 2004.

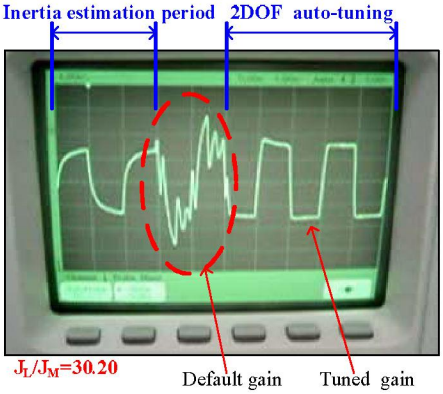

Fig. 12. Speed responses tested by default gains and tuned gains after load estimation.

[9] E. Chiricozzi , F. Parasiliti , M. Tursini and D. Q. Zhang, "Fuzzy self-tuning PI control of PM synchronous motor drives," *Int. J. Electronics*, vol. 80, no. 2, pp. 211-221, 1996.

[10] K. Inoue, T. Izumi, E. Hiraki, and M. Nakaoka, "A DC brushless servo drive system controlled by fuzzy-logic based auto-tuning implementation," International *IEEE/IAS Conference on Industrial Automation and Control: Emerging Technologies,* pp. 208-212, 22-27 May 1995.

[12] C. Rossi and A. Tonielli, "Robust control of permanent magnet motors: VSS techniques lead to simple hardware implementations," *IEEE Trans. on Industrial Electronics*, vol. 41, pp. 451-460, 1994.

[13] K. Cheng, S.-Y. Lin and Y.-Y. Tzou, "On-line auto-tuning of a DSP-controlled BLDC servo drive," *2001 IEEE 32nd Annual Power Electronics Specialists Conference,* vol. 3, pp. 1683-1688, 17-21 June 2001.

[14] Y.-Y. Tzou and Y.-F. Lin, "Auto-tuning control of self-commissioning electric drives," *23rd International Conference on Industrial Electronics, Control and Instrumentation,* vol. 2, pp. 483-487, 9-14 Nov. 1997.

[15] G. Ellis, *Control System Design Guide*, Academic Press, San Deigo, California, USA, 2000.

[16] N. Hur, K. Nam, and S. Won, "A two-degrees-of-freedom current control scheme for deadtime compensation," *IEEE Trans. on Industrial Electronics*, vol. 47, pp. 557-564, 2000.